

An AMC Based Metasurface Patch Antenna for C-Band and X-Band Applications

Diptiranjana Samantaray
Electronics Engineering
IIT(BHU), Varanasi
Varanasi, India

drsamarantay.rs.ece17@iitbhu.ac.in

Somak Bhattacharyya
Electronics Engineering
IIT(BHU), Varanasi
Varanasi, India

somakbhattacharyya.ece@iitbhu.ac.in

Abstract— A low-profile, efficient and directive gain enhanced antenna on an artificial magnetic conductor (AMC) reflector has been proposed in this paper. The AMC based metasurface antenna (MSA) has been formed by incorporating the CPW-fed slotted patch antenna along with a 5×5 order metasurface (MS). The slotted patch and the AMC reflector have been designed over FR4 dielectric and separated by a layer of Teflon, thereby acting as a superstrate. This antenna has fractional bandwidths of 11.6 %, 5.3 %, and 7% at three frequencies, such as 4.13 GHz, 8.80 GHz, and 12.01 GHz respectively. The antenna achieves the realized gain of 10.2 dBi at 12.4 GHz. The antenna provides directional radiation characteristics in both the E- and H-planes. The proposed prototype can be used for WLAN applications, medical supervision, satellite communication, and defence applications in the C and X-bands.

Keywords— Microstrip, slotted patch, CPW-fed, metasurface, artificial magnetic conductor (AMC).

I. INTRODUCTION

Because wireless communication applications necessitate multiband to wideband characteristics, research into the design of highly directive gain enhanced broadband antennas for WLAN and X-band applications is gaining momentum [1–5]. Recently, various technologies, such as the use of parasitic elements and inserting slots in the radiating structure, have been implemented to improve the performance of the impedance bandwidth of the antenna [4]–[8]. Several feeding methodologies, such as microstrip line fed, inset fed, edge fed, coaxial probe fed, CPW-fed, and so on, have been used in antenna structures to improve antenna features [3–13]. The CPW-fed slot antenna is more effective and prominent for multiband to wideband characteristics in wireless applications; however, the antenna gain becomes low [8] – [11]. The artificial magnetic conductor (AMC) structure is a type of high impedance metasurface (MS) that is widely used to improve antenna performance in radiation reflectors [8] – [10]. It is an electromagnetic periodic structure created by humans in which the electromagnetic characteristics of the reflecting plane wave are in phase over a specified frequency range [8] – [10].

A portable, efficient, high gain, triple band, and directional AMC based MS antenna is discussed in this paper. The proposed antenna has been integrated with a CPW-fed slotted patch antenna along with a 5×5 order MS. The radiating patch has been placed at the top position of the first dielectric, whereas the MS layer has been placed on the back side of the second dielectric. The MS antenna is frequency selectable between 4.13 GHz, 8.80 GHz, and 12.01 GHz, with a maximum return loss of

36 dB at 12.01 GHz. At three operational frequencies, this antenna gives fractional bandwidths of 11.6 %, 5.3 %, and 7%, with a maximum achievable gain of 10.2 dBi at 12.4 GHz. In both the E- and H-planes, the prototype exhibits directional radiation features.

II. DESIGN OF METASURFACE ANTENNA

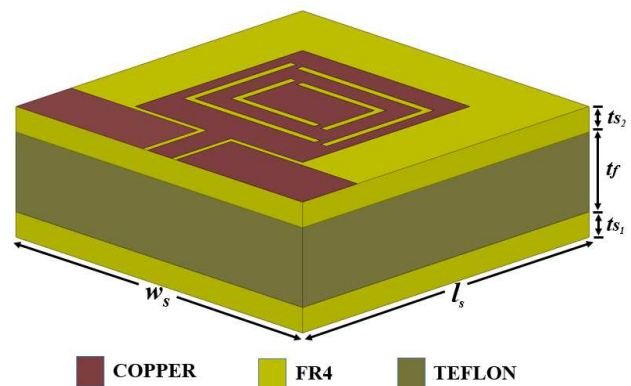


Fig. 1. The 3D view of the proposed AMC based metasurface structure.

The proposed antenna is made up of a CPW-fed slotted patch as the radiating element and a 5×5 order MS. The patch and AMC reflector are designed on two different FR4 dielectric substrates (relative permittivity of 4.4 and loss tangent of 0.025) with a mutual separation of 5 mm thick Teflon (loss tangent = 0.001 and relative permittivity = 2.1) layer. The MS unit cell is designed with a centre patch surrounded by a square ring shaped patch. Fig. 1 illustrates a 3D schematic view of the proposed AMC-based MS structure. In addition, the top and bottom views of the proposed prototype are depicted in Figs. 2(a) and 2(b), respectively. Ansys HFSS [14] has been used for analysis and optimization of the proposed prototype. Table I shows the parametrically optimized dimensions of the proposed design.

The proposed CPW-fed patch is designed in three stages. The conventional patch design steps with various modifications are depicted in Fig. 3, and their respective return loss characteristics are depicted in Fig. 4. Initially, a 14×14 mm² square patch was used as a radiating element, which is depicted in Fig.3 as CASE-I. This simple patch operates at 9.74 GHz over a narrow bandwidth between 9.52 GHz and 10.00 GHz.

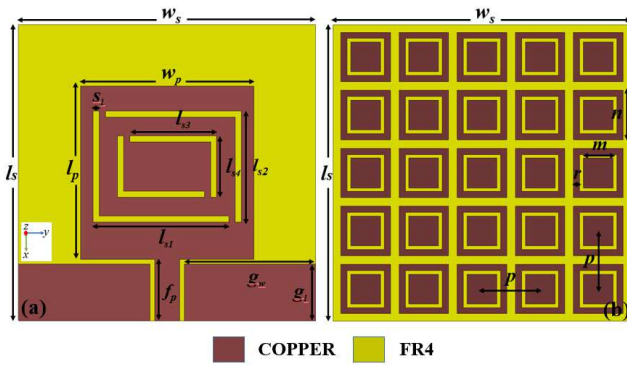


Fig. 2. Schematic view of the proposed AMC based metasurface antenna with (a) top and (b) bottom views.

TABLE I. THE OPTIMIZED GEOMETRICAL DIMENSIONSS OF THE AMC BASED MS ANTENNA

Antenna elements	Dimension (mm)	Antenna elements	Dimension (mm)
$w_s = l_s$	24	l_{s2}	9
$w_p = l_p$	14	l_{s3}	7
$ts_1 = ts_2$	1.6	l_{s4}	5
t_f	5	s_l	0.5
f_p	5	n	4
g_w	10.6	m	2.4
g_l	4.6	r	1
l_{s1}	11	p	0.7

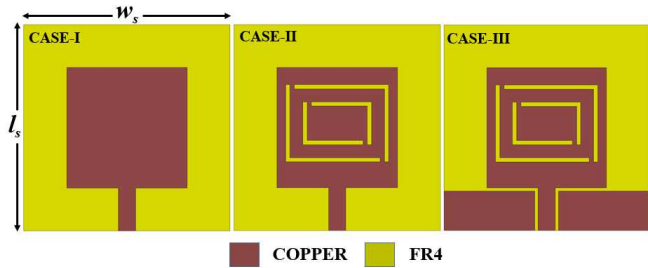


Fig. 3. Design steps of the conventional patch with different modifications.

Later, parasitic L-shaped slot elements have been included in the patch to improve the frequency of operations and bandwidth. The slotted patch in CASE-II of Fig.3 operates at two frequency ranges: 3.84 GHz-3.95 GHz and 9.88 GHz-10.23 GHz, with a maximum return loss of 20 dB at 10.03 GHz. Furthermore, CPW-feed has been combined with the slotted patch to improve antenna performance, as shown in CASE-III of Fig.3. Again, the antenna performs at dual frequency regions while the antenna performance undergoes enhancement in terms of bandwidth and return loss. The CPW-fed patch antenna produces enhanced bandwidths from 3.92 GHz-4.61 GHz and 9.11 GHz-9.44 GHz with maximum return loss of 29 dB at 4.36 GHz. Next, a 5×5 order MS has been incorporated with a CPW-fed slotted patch in which the MS has been placed below the radiating patch with a different FR4 dielectric. A layer of 5 mm thick Teflon dielectric has been placed in between two FR4 dielectrics, forming a superstrate structure.

The structure of the designed 3D view of the AMC unit cell has been shown in Fig. 5 (a). It consists of a centered patch surrounded by a square shaped ring. Here, the equivalent LC parallel resonance can be formed by adjusting the parameters of the AMC unit cell. Periodic boundary conditions are used to excite the unit cell using commercial Ansys HFSS software [14]. By studying the reflection and transmission properties of the periodic unit cell, a detailed investigation of the electromagnetic behavior of effective permittivity and permeability of the MS layer has been carried out. In Fig. 5(b) and Fig. 5(c), the real and imaginary parts of the same have been represented, respectively. In the frequency bands of 1-3.8 GHz and 8.8-11 GHz, the AMC-based MS layer operates as a left-handed material.

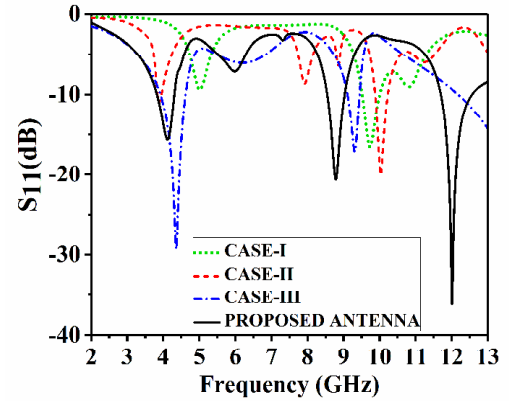


Fig. 4. Plot of S_{11} (dB) with respect to frequency of the different antenna configurations shown in Fig. 3.

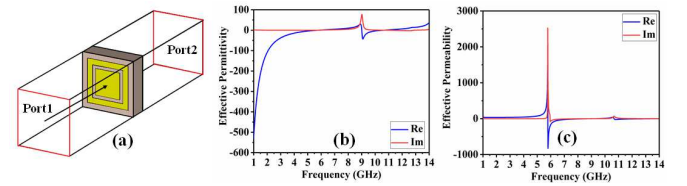


Fig. 5. (a) The 3D view (b) Effective permittivity and (c) Effective permeability of unit cell.

The homogeneity properties of the metasurface have been taken into consideration when designing the AMC unit cells. The incorporation of the AMC layer just below the radiating patch arranged in superstrate shape enhances the performance of the antenna. The reflection characteristics of the proposed AMC-based MS antenna have also been compared with those of other designed antennas, as highlighted in Fig. 4. The designed prototype operates in three distinct frequency bands viz., 3.82-4.30 GHz, 8.55-9.02 GHz and 11.71-12.56 GHz with the maximum fractional bandwidths of 11.6%, 5.3% and 7% respectively.

III. SIMULATED RESULTS

The reflection coefficient characteristics of the proposed AMC based MS antenna along with the conventional patch antenna have been shown in Fig. 6. The CPW-fed radiating patch works over two frequency bands ranging from 3.92-4.61 GHz and 9.11-9.44 GHz with maximal return loss of 29 dB at 4.36 GHz.

The conventional patch antenna possesses the fractional bandwidths of 15% and 3.5% at 4.36 GHz and 9.32 GHz respectively. Further, the performance of the conventional patch has been significantly improved by incorporating a 5×5 order AMC layer with Teflon in superstrate configuration. The loading of the AMC layer results in triple-band response of the antenna operating over the bands 3.82-4.30 GHz, 8.55-9.02 GHz and 11.71-12.56 GHz with the respective fractional bandwidths of 11.6%, 5.3% and 7% at 4.13 GHz, 8.80 GHz and 12.01 GHz as evident from Fig. 6. The maximum return loss of 36 dB has been achieved at 12.01 GHz.

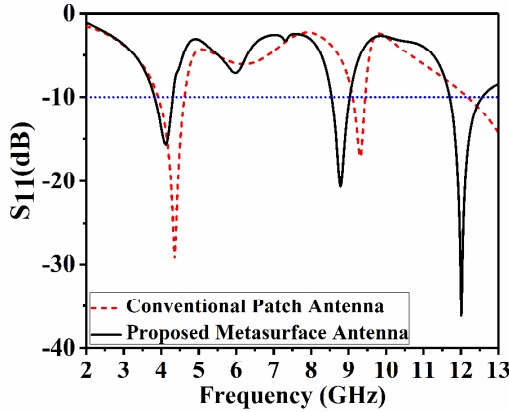


Fig. 6. Plot of S_{11} (dB) with respect to frequency of the proposed antenna prototype.

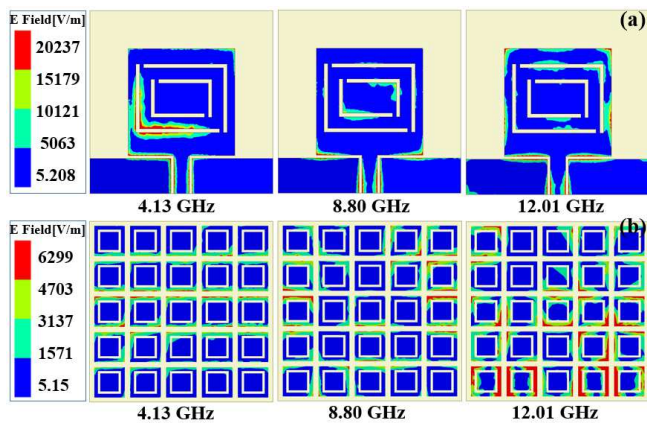


Fig. 7. Electric field distributions of the proposed antenna structure at 4.13 GHz, 8.80 GHz and 12.01 GHz at different surfaces.

The electric field distributions of the CPW-fed patch and the MS layer at three distinct operating frequencies, viz., 4.13 GHz, 8.80 GHz, and 12.01 GHz, are shown in Fig. 7(a) and Fig. 7(b) respectively. It is noticed that the field distribution is greatest around slots, as well as the patch and unit cell surface interfaces of the MS. The surface current distributions at 4.13 GHz, 8.80 GHz, and 12.01 GHz for the top surface of the radiating patch and the bottom AMC layer have also been studied and are shown in Fig. 8(a) and Fig. 8(b) respectively. They are denser in the area between the patch's surface interface and the CPW feed. The directions of surface currents at the interface of the unit cells are parallel to each other, forming a magnetic coupling between the adjacent unit cells, as shown in Fig. 8(b). This phenomenon also helps to achieve the best impedance matching at 12.01 GHz.

The frequency response of the realized gain of the suggested prototype is depicted in Fig. 9. The proposed MS antenna achieves maximum realized gains of 4.3 dBi, 3.6 dBi, and 10.2 dBi at the operating frequency bands of 3.82-4.30 GHz, 8.55-9.02 GHz, and 11.71-12.56 GHz, respectively. At 12.4 GHz, a maximum gain of 10.2 dBi has been achieved.

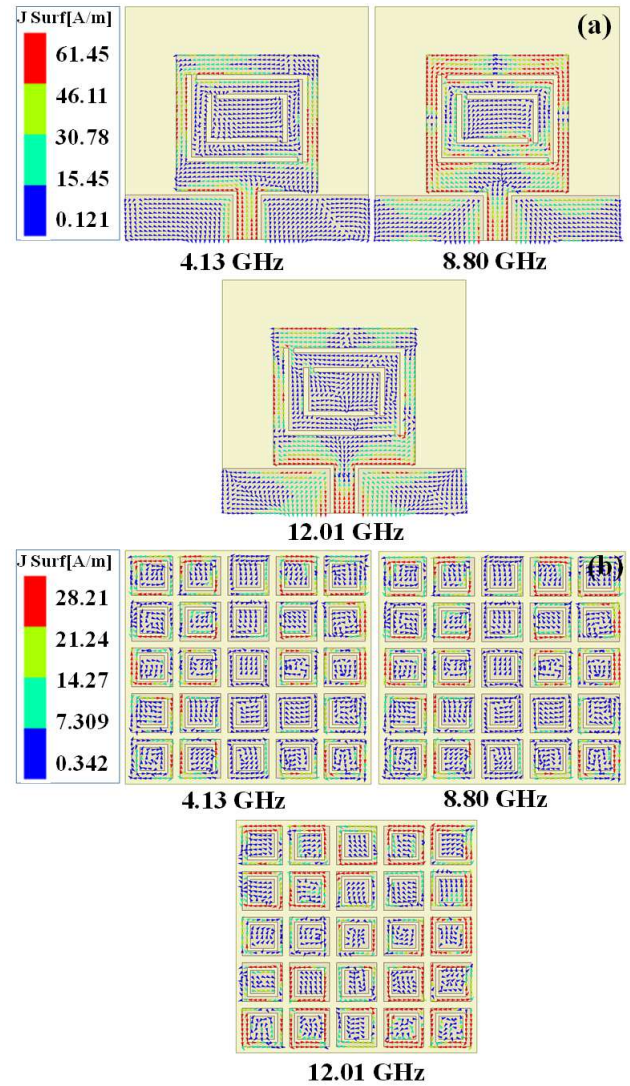


Fig. 8. Surface current of the proposed prototype at 4.13 GHz, 8.80 GHz and 12.01 GHz.

The analyses of co-polarized and cross-polarized radiation characteristics along the E- and H-planes of the proposed AMC-based CPW-fed MS antenna are depicted in Fig. 10(a) and Fig. 10(b) at 4.13 GHz, 8.80 GHz, and 12.01 GHz, respectively. It is observed that at 4.13 GHz and 8.80 GHz, the antenna radiates along the boresight direction both in the E- and H-planes. On the contrary, the property of directed radiation was realized at 12.01 GHz. Additionally, it has been shown that the cross-polarized radiation level is significantly lower than the co-polarized radiation level at all operating frequencies.

A comparison study of the proposed AMC-based MS antenna with other reported MS antenna designs is shown in Table II. It can be seen that the proposed prototype outperforms the

reported ones in terms of gain enhancement and bandwidth across different frequency bands.

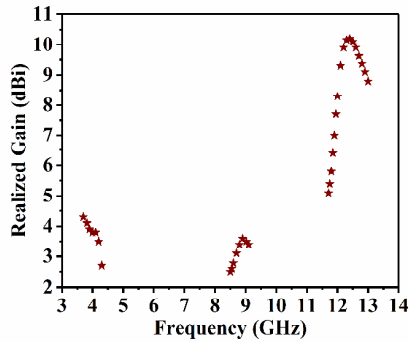


Fig. 9. Plot of the realized gain (dBi) of the proposed prototype at different operating frequencies.

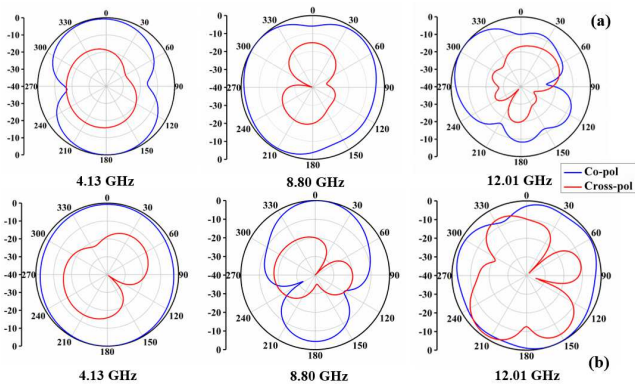


Fig. 10. Radiation patterns in the (a) E-plane and (b) H-plane at frequencies of 4.13 GHz, 8.80 and 12.01 GHz.

TABLE II. A COMPARATIVE STUDY OF PROPOSED AMC BASED MS ANTENNA WITH REPORTED MS ANTENNAS

Antenna Literature	Operation Frequencies of the antenna (GHz)	Fractional Bandwidth (%)	Maximum Gain (dBi)	Radiating Element
Lin <i>et al.</i> [15]	1.24-1.52, 1.49-1.65	2, 1	7	Dipole Antenna
Ghosh <i>et al.</i> [16]	3.33-3.39, 5.92-6.2, 9-9.2	1.8, 4.6, 2.2	11.1	Rectangular Patch
Ghosh <i>et al.</i> [17]	3.7-4.1, 6.1-6.2, 9-9.2	8.2, 4.5, 3.5	7.5	Slotted patch
Sarkar <i>et al.</i> [18]	0.9-0.93, 2.43-2.45	5.2, 2	6.25	Circular patch
Paracha <i>et al.</i> [19]	1.56-1.59, 2.43-2.47	1.8, 0.7	5.1	Pentagonal patch
Proposed Design	3.82-4.30, 8.55-9.02, 11.71-12.56	11.6, 5.3, 7	10.2	Square patch

IV. CONCLUSIONS

This paper presents a new, low-profile, and efficient AMC-based metasurface antenna for C- and X-band applications. A slotted patch and a 5×5 array of periodic unit cells arranged in superstrate configuration are included in the proposed model. The antenna operates at three different frequencies, with fractional bandwidths of 11.6 %, 5.3 %, and 7 % at 4.13 GHz, 8.80 GHz, and 12.01 GHz, respectively. The antenna exhibits

directional radiation characteristics in both the E- and H-planes, with a maximum realized gain of 10.2 dBi at 12.4 GHz. This antenna can be used in C-band and X-band applications such as WLAN, medical supervision, satellite communication, and defence.

REFERENCES

- [1] Liu, W. E. I. Z., Chen, N., Qing, X., Shi, J., & Lin, F. H., "Miniaturized Wideband Metasurface Antennas," *IEEE Transactions on Antennas and Propagation*, vol. 65, no. 12, pp. 7345-7349, 2017.
- [2] W. Liu, Z. N. Chen, and X. M. Qing, "Metamaterial-based low-profile broadband aperture-coupled grid-slotted patch antenna," *IEEE Trans. Antennas Propagation*, vol. 63, no. 7, pp. 3325-3329, Jul. 2015.
- [3] D Samantaray, S Bhattacharyya, K. V. Srinivas, "A modified fractal-shaped slotted patch antenna with defected ground using metasurface for dual band applications," *International Journal of RF and Microwave Computer-Aided Engineering*, vol. 29, no. 12, pp. 1-9, Dec. 2019.
- [4] J. Wu, S. Yang, Y. Chen, S. Qu, and Z. Nie, "A low profile dual-polarized wideband omnidirectional antenna based on AMC reflector," *IEEE Transaction Antennas Propagation*, vol. 65, no. 1, pp. 368-374, Jan. 2017.
- [5] Y. F. Cao, S. W. Cheung, and T. I. Yuk, "A multiband slot antenna for GPS/WiMAX/WLAN systems," *IEEE Transaction Antennas Propagation*, vol. 63, no. 3, pp. 952-958, Mar. 2015.
- [6] A. T. Abed, M. S. J. Singh, and M. T. Islam, "Compact fractal antenna circularly polarized radiation for Wi-Fi and WiMAX communications," *IET Microwave Antennas Propagation*, vol. 12, no. 14, pp. 2218-2224, Nov. 2018.
- [7] D Samantaray, S Bhattacharyya, "A Metasurface Based Gain Enhanced Dual Band Patch Antenna Using SRRs With Defected Ground Structure," *Radio Science*, vol. 56, issue 2, article no. 2020RS007192, Feb. 2021.
- [8] H. Malekpoor and S. Jam, "Improved radiation performance of low profile printed slot antenna using wideband planar AMC surface," *IEEE Trans. Antennas Propagation*, vol. 64, no. 11, pp. 4626-4638, Nov. 2016.
- [9] S. Yan, P. J. Soh, and G. A. E. Vandenbosch, "Low-profile dual-band textile antenna with artificial magnetic conductor plane," *IEEE Trans. Antennas Propagation*, vol. 62, no. 12, pp. 6487-6490, Dec. 2014.
- [10] Q. Liu, H. Liu, W. He, and S. He, "A low-profile dual-band dual-polarized antenna with an AMC reflector for 5G communications," *IEEE Access*, vol. 8, pp. 24072-24080, Jan. 2020.
- [11] M Jha, D Samantaray, S Bhattacharyya, "A THz antenna with sandwiched metasurface for quadband application," *Optics Communications*, vol. 493, pp. 1-10, Aug. 2021.
- [12] T. Li and Z. N. Chen, "A Dual-Band Metasurface Antenna Using Characteristic Mode Analysis," in *IEEE Transactions on Antennas and Propagation*, vol. 66, no. 10, pp. 5620-5624, October 2018.
- [13] D. Samantaray and S. Bhattacharyya, "A Gain-Enhanced Slotted Patch Antenna Using Metasurface as Superstrate Configuration," in *IEEE Transactions on Antennas and Propagation*, vol. 68, no. 9, pp. 6548-6556, Sept. 2020.
- [14] Ansys Electronics Desktop, R1, 2019, ANSYS Corporation.
- [15] J. Lin, Z. Qian, W. Cao, S. Shi, Q. Wang and W. Zhong, "A Low-Profile Dual-Band Dual-Mode and Dual-Polarized Antenna Based on AMC," in *IEEE Antennas and Wireless Propagation Letters*, vol. 16, pp. 2473-2476, 2017.
- [16] A. Ghosh, V. Kumar, G. Sen, and S. Das, "Gain enhancement of triple-band patch antenna by using triple-band artificial magnetic conductor," *IET Microwave Antennas Propagation*, vol. 12, no. 8, pp. 1400-1406, Jul. 2018.
- [17] A. Ghosh, T. Mandal, and S. Das, "Design of triple band slot-patch antenna with improved gain using triple band artificial magnetic conductor," *Radioengineering*, vol. 25, no. 3, pp. 442-448, Sep. 2016.
- [18] S. Sarkar and B. Gupta, "A Dual-Band Circularly Polarized Antenna With a Dual-Band AMC Reflector for RFID Readers," in *IEEE Antennas and Wireless Propagation Letters*, vol. 19, no. 5, pp. 796-800, May 2020.
- [19] K. N. Paracha et al., "A Low Profile, Dual-band, Dual Polarized Antenna for Indoor/Outdoor Wearable Application," in *IEEE Access*, vol. 7, pp. 33277-33288, 2019.